

Structural and Reactivity Properties of Finite Length Cap-Ended Single-Wall Carbon Nanotubes

Jin Zhao and Perla B. Balbuena*

Department of Chemical Engineering, Texas A&M University, College Station, Texas 77843

Received: December 3, 2005; In Final Form: January 10, 2006

The reaction of C_2 with growing single-wall carbon nanotubes of different chiralities is investigated using density functional theory. It is found that the energy of the frontier orbitals for (5,5) and (6,6) armchair carbon nanotubes exhibits periodic behavior with an increasing number of carbon atoms in the nanotube. Such periodic behavior induces oscillations in the reaction energy released by adsorption of C_2 to the nanotube open edge. In contrast, the energy of the frontier orbitals of the (6,5) chiral tube remains constant as the number of C atoms increases, and the same stability is observed in the adsorption energy. It is suggested that this may be one of the reasons for the low percent of armchair single-wall carbon nanotubes found in the experimental synthesis.

1. Introduction

Single-wall carbon nanotubes (SWNTs) are synthesized by a variety of methods, among them by catalytic decomposition of a C-containing precursor gas over metal nanoparticles^{1–3} at elevated temperatures (in the order of 1000 K) and pressures from 1 to ~ 100 atm. The growth mechanism has been intensively examined by theoretical and experimental methods.⁴ One of the most important aspects that are not yet understood is related to the selective growth of tubes of specific chiralities under certain synthesis conditions.⁵ For example, in the CoMoCAT process, where CO is decomposed over Co catalysts deposited in a Mo-oxide support, the most abundant SWNTs found include the chiral (6,5) and (7,5), and only a small percent of armchair tubes is found.^{6–8}

In recent work we have examined details of the growth process using classical molecular dynamics simulations and a reactive force field.^{9,10} Our simulations identified five stages in the growth mechanism: (1) The precursor decomposes on the metal catalyst surface and C atoms diffuse inside the metal nanoparticle. (2) C dissolution reaches a degree of saturation determined by the metal–metal and metal–substrate interactions and starts to precipitate on the surface forming isolated or interconnected short chains. (3) Fullerene-type structures start to form on the surface. (4) A cap is formed. (5) The nanotube grows. One of the more accepted mechanisms of SWNT growth is based on the assumption that a fullerene-type cap lifts off from the metal catalyst (as that described in our proposed fourth step) and its continued growth evolves into a cap-ended nanotube. This mechanism has been discussed on the basis of experimental and theoretical investigations.^{11,12} Details of the nucleation process of the nanotube given by the formation of the cap and its lifting from the catalyst surface are complex. The specific structural and reactivity properties of the cap-ended nascent nanotube are most likely responsible for its survival probability, because the edges will be those attracting C_2 or other short C-chains, as suggested by the interesting chemistry of fullerenes and SWNTs recently reviewed.¹³

In this work we analyze the electronic and reactive properties of cap-ended carbon nanotubes: armchair (5,5) and (6,6), and the (6,5), one of the chiral tubes more frequently found in the Co–MoCAT synthesis process.¹⁴ The energies, shapes, and reactivity properties of the highest occupied and lowest unoccupied molecular orbitals (HOMO and LUMO, respectively) are investigated as a function of the number of C atoms in the cap-ended carbon nanotube. In addition, the evolution of the LUMO and HOMO of the complex formed upon adsorption of a C_2 radical to the nanotube edge and the corresponding adsorption energies are investigated.

2. Model Design and Calculation Details

The present calculations are based on the hypothesis that the caps of (5,5), (6,6) and (6,5) carbon nanotubes have been formed in the fourth step of catalyzed nanotube growth, as outlined in

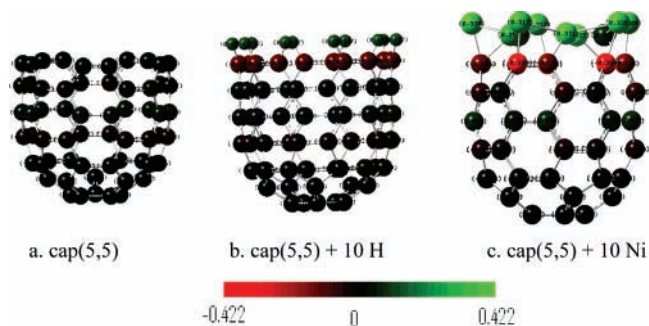


Figure 1. Charge distribution in the cap atoms; the color of each atom represents its charge as shown in the scale.

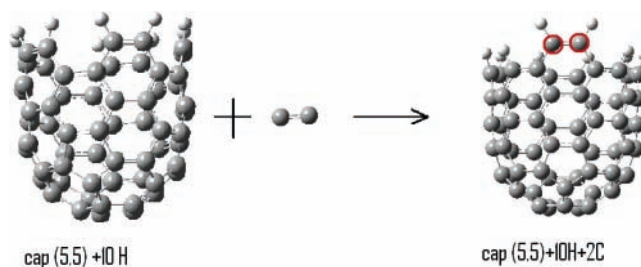


Figure 2. Reaction of a cap with C_2 .

* Corresponding author. E-mail: balbuena@tamu.edu.

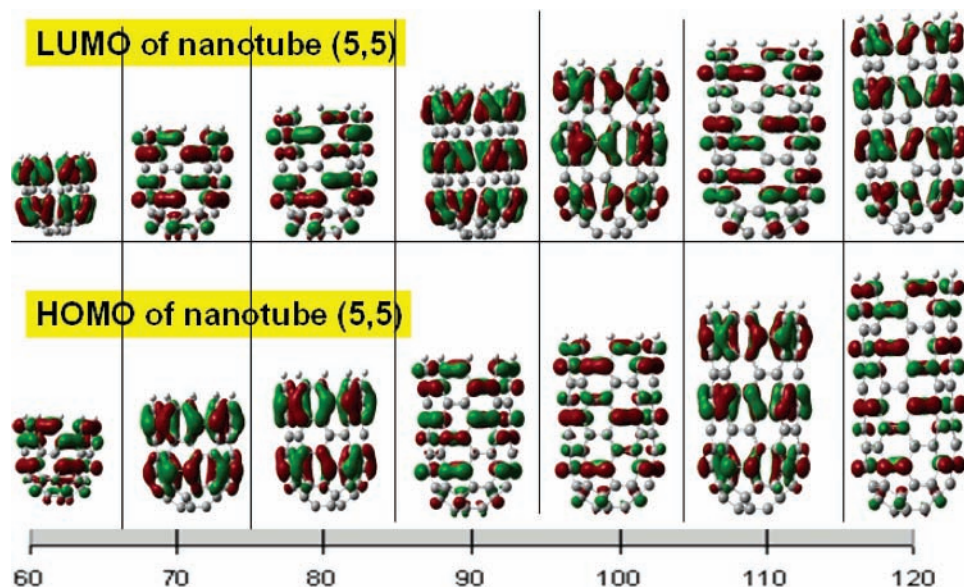


Figure 3. HOMO and LUMO of caps (5,5) of increasing number of atoms as predicted by B3LYP/6-31G.

the Introduction. Thus, we intend to perform a comparative study to determine which cap may be easier to grow into a nanotube, based on their reactive properties.

To design our computational model, we first studied the distribution of electronic charge for a simple cap terminated by hydrogen atoms at its open end, and for a cap where the carbon atoms at the open end are bonded to Ni atoms, as shown in Figure 1. The distribution of electronic charge was determined after geometry optimizations using the density functional theory B3LYP method and 6-31G basis set. In both cases it was found that the carbon atoms at the open end are negatively charged; that is to say, both Ni atoms and H atoms act as electron donors.

Although the effect of the catalyst metal cluster on the growth of nanotube is quite complex, here we assume that one of the roles of the metal atoms is to provide electrons to the cap in the same way as hydrogen atoms do. On the basis of this simplification, to reduce the computational expenses, we study the reactive properties of different caps terminated by hydrogen atoms.

Our previous classical molecular dynamics simulations^{9,10} suggested that when a cap starts growing into a nanotube, short carbon chains or branched chains react with the open edge of the growing cap, forming carbon rings that would become part of the cap if the cap is stable; otherwise they would break into shorter chains that would try to form new rings again. Thus the growth of the cap is a very complex process with numerous possibilities. Yet here we just discuss the simplest reaction path: a carbon dimer reacts with the cap, contributing to the cap growth. We use B3LYP/6-31G to calculate the energy change of this reaction for different caps as shown by

$$\Delta E = E_{\text{new-cap}} - E_{\text{cap}} - E_{\text{C}_2} \quad (1)$$

Because the open end is saturated by H atoms (Figure 2), eq 1 implies that two H atoms are displaced by the C atoms, but the process of removal of the H atoms and their posterior attachment to the new bonded C2 is not addressed by our calculations. The calculation scheme is illustrated in Figure 2.

Full geometry optimizations were performed using density functional theory, B3LYP/6-31G. All calculations were done using the program Gaussian 03.¹⁵

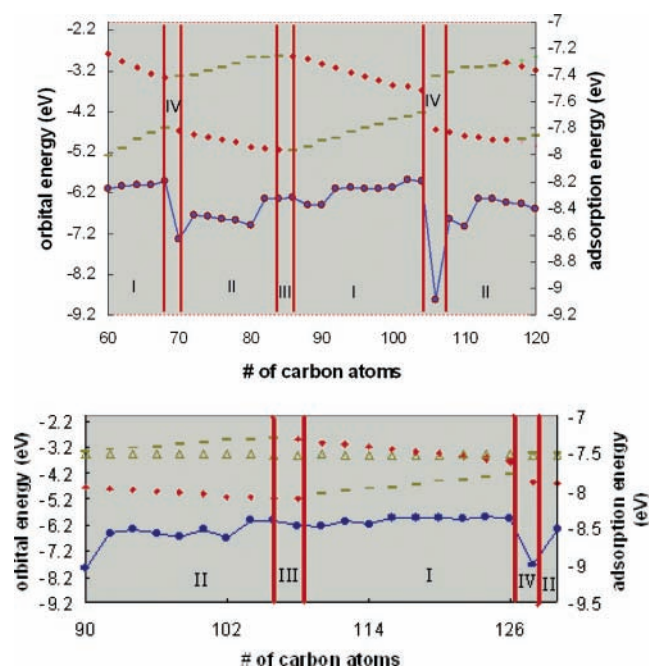


Figure 4. Energetic behavior of nanotubes vs the number of C atoms for armchair nanotubes. Top: the upper line corresponds to the LUMO energy and the middle line to the HOMO energy of a (5,5) nanotube, both measured in the left vertical axis. Red diamonds indicate antisymmetric and green short lines symmetric orbitals. The adsorption energy is given by the solid blue line, measured on the right vertical axis. The vertical lines separate regions of a given type of behavior, as explained in Table 1. Bottom: for the (6,6) carbon nanotube, the top line is the second lowest unoccupied molecular orbital (diamonds and short lines), followed by the LUMO (triangles), HOMO (third line: diamonds and short lines), and adsorption energy (solid blue line).

3. Results and Discussion

The structure of armchair carbon nanotubes is highly symmetric. Our calculations indicate that increasing the number of carbon atoms in the nanotube, the shape of the frontier LUMO and HOMO molecular orbitals changes periodically, as illustrated in Figure 3 for (5,5) cap-ended nanotubes.

Figure 4 (top) illustrates the periodic variation of the energy of the frontier orbitals for the (5,5) carbon nanotube. Such oscillations in the orbital energies are in qualitative agreement

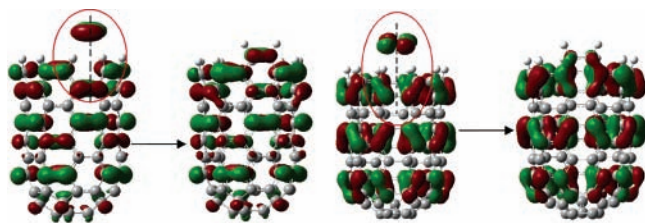


Figure 5. Overlap between π orbitals of the cap and C_2 .

with those reported by Matsuo et al.,¹⁶ who calculated the HOMO and LUMO levels in open-ended (5,5) nanotubes. Also Tomanek et al. showed the periodic dependency on the tube length of the electronic structure of open-ended ($n,0$) zigzag carbon nanotubes and that of their frontier molecular orbitals.¹⁷ We have categorized the energetic behavior of the (5,5) armchair

cap-ended SWNT into four classes: I, II, III, and IV, which are defined by the symmetry properties of the LUMO and HOMO orbitals. Figure 4 shows that in the first period (starting with 60 C atoms), the antisymmetric orbital is the LUMO and the gap between HOMO and LUMO decreases with the increasing number of carbon atoms, until there are 68 atoms and the gap reaches the smallest value of 1.2 eV. At this point, the symmetric orbital becomes the LUMO and the HOMO–LUMO gap begins to increase. We call this point the switching point. In the second period I (Figure 4, top), the qualitative behavior is similar: the antisymmetric orbital is the LUMO and the symmetric the HOMO, and the gap decreases, reaches about 1.0 eV at 98 atoms, and keeps decreasing until it reaches 0.58 eV at 108 C atoms. It is known that infinite-length armchair nanotubes are metallic and their HOMO–LUMO gap should

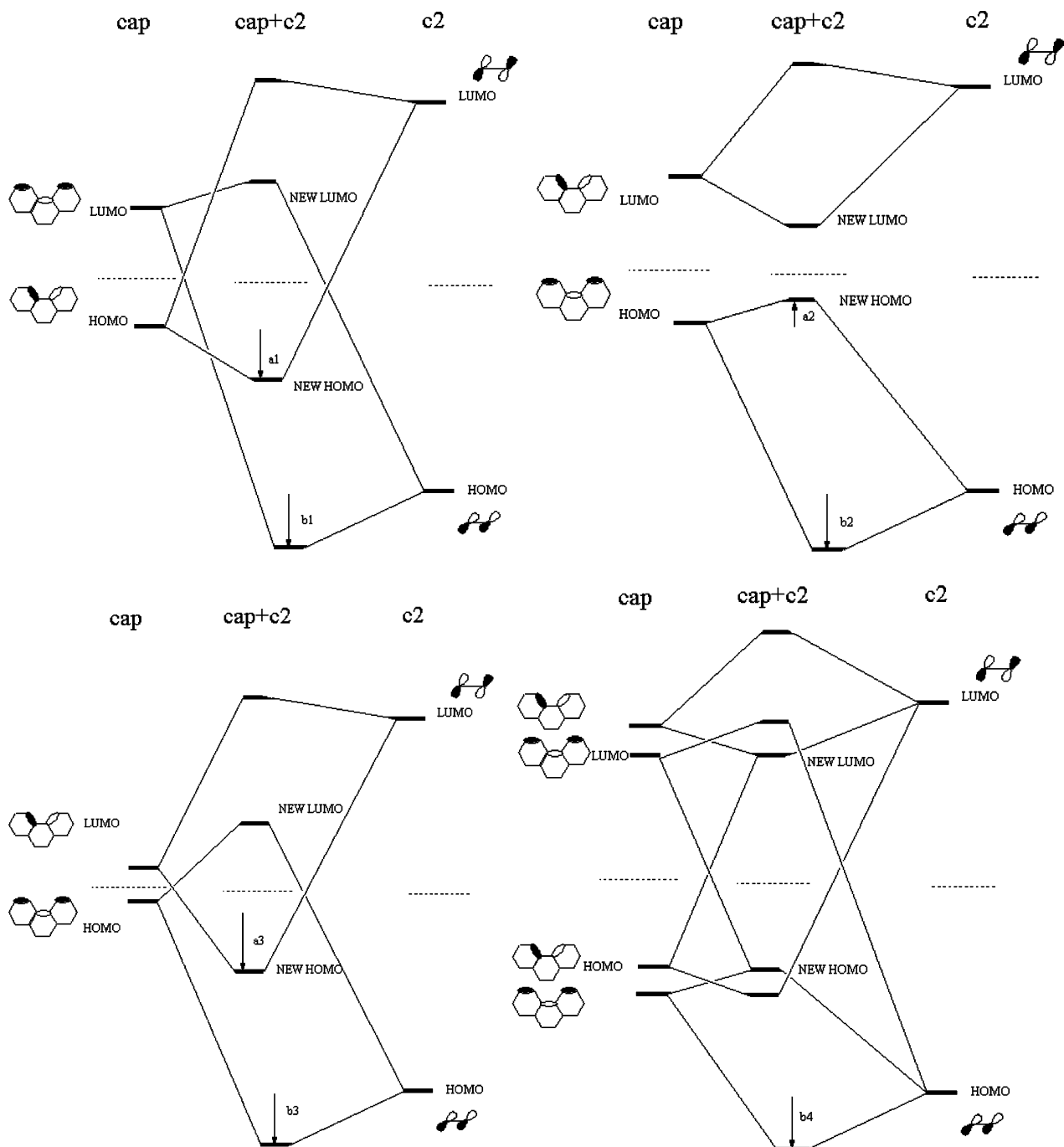


Figure 6. Schematic description of the overlap of π orbitals in cap (5,5) with those of C_2 . Diagrams correspond to symmetry regions indicated in Table 1 and Figure 4 (top): top left, region II; top right, region I; bottom left, region IV; bottom right, region III.

TABLE 1: Correlation between Symmetry Properties of the HOMO and LUMO Orbitals and the Reaction Energy of C₂ and the Growing (5,5) Carbon Nanotube^a

region in Figure 4	symmetry (S: symmetric; A: antisymmetric)				energy decrease because of π orbitals overlap	calcd reaction energy/eV
	LUMO	HOMO	LUMO	HOMO		
II	S	A	S	A	a1 + b1	-8.6 to ~-8.4
I	A	S	A	S	b2 - a2	-8.3 to ~-8.2
IV	A	S	S	A	a3 + b3	-9.0 to ~-8.6
III	S	A	A	S	b4	~-8.3 eV

^a The quantities a1, b1, a2, b2, b3, and b4 are shown in Figure 6.

disappear, but the gap still exists in finite-length armchairs. This length dependence of the HOMO–LUMO gap may explain the shift of the switching point. Figure 3 shows that the HOMO and LUMO orbitals of nanotubes with 60 atoms, 90 atoms, and 120 C atoms have identical shapes, and those of the nanotube with 80 C atoms are identical with the one of 110 C atoms, but because of the shift of the switching point, the orbitals of the (5,5) cap-ended nanotube with 70 atoms are not identical to those of the 100 atoms tube.

The reaction energy as a function of the number of carbon atoms has also a defined behavior in each region, as shown in Figure 4. In regions I, the LUMO energy decreases and the HOMO increases, and the opposite behavior takes place in regions II. In region IV, the HOMO energy reaches a maximum, and the LUMO a minimum, these points are expected to be of high reactivity,¹⁸ as reflected by the peaks in the adsorption energy.

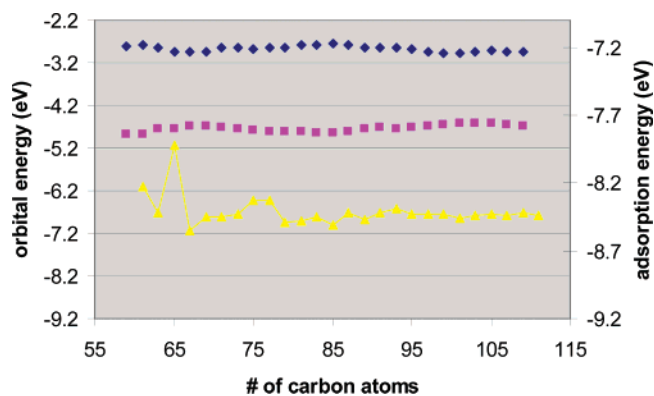
The HOMO and LUMO energies of the larger diameter (6,6) armchair carbon nanotube (Figure 4, bottom) also display periodic behavior, although with a larger oscillation period.

To investigate the details of the reaction, we analyze the orbitals of the reactants and products. C₂ has σ_g , σ_u , π_u , and π_g orbitals, which can overlap with the corresponding cap orbitals. Because the cap σ orbitals are all quite low in energy and totally occupied, there is a decrease in the orbital energy because of the σ orbitals overlap, which is similar for caps (5,5) with different numbers of carbon atoms. On the other hand, the cap π orbital that is symmetric with respect to an axis perpendicular to the C–C bond in C₂ can overlap with the π_u of C₂, whereas those that are antisymmetric with respect of the same axis can overlap with the π_g orbital of C₂, as shown in Figure 5. As illustrated in Figure 4, the energy of the symmetric and antisymmetric π orbitals and their occupancy state changes with increasing number of carbon atoms in the cap.

Figure 6 schematically illustrates the energies of the LUMO and HOMO of the original cap, and those of C₂. The central values correspond to the energies of the two lowest unoccupied and the two highest occupied molecular orbitals of the product, cap+C₂.

We designate the energy differences between the highest occupied orbital of the old and the new tube as *a*, and that between the second highest occupied molecular orbital of the new tube and HOMO of C₂ as *b*. In Figure 6, top left, both of the two occupied orbitals of the new tube have lower energy than that of the reactant, so the energy decreases because of the overlap of π orbitals in an amount equal to a1 + b1. The energy decrease due to overlap of the π orbitals in the other cases illustrated by Figure 6 are described in Table 1.

The periodic behavior shown by the orbital energies explains the corresponding variations of the reaction energy with the increasing number of carbon atoms in the cap-ended

**Figure 7.** Energetic behavior of the (6, 5) nanotube frontier orbitals vs the number of C atoms: top, LUMO; middle, HOMO; bottom, adsorption energy.**TABLE 2: Adsorption Energy To Incorporate a C₂ Radical to Different Nanotubes**

	adsorption energy/eV	average value/eV
(5,5)	-8.23 to ~-9.08	-8.36
(6,5)	-8.39 to ~-8.44	-8.43
(6,6)	-8.35 to ~-9.03	-8.47

(5,5) nanotube; such oscillatory behavior would make it sometimes easier (or more difficult) to add more rings to the cap.

In contrast, the structure of the chiral (6,5) is less symmetric and no obvious periodic properties are found. The energy of the HOMO and LUMO orbitals does not change while the number of carbon atoms in the nanotube increases, as illustrated by Figure 7. Regarding the reaction energy, when the number of carbon atoms is rather small, it changes irregularly, but after the number of carbon atoms reaches a certain value, the reaction energy also remains constant with the increasing of number of carbon atoms. We choose to ignore the small binding energy occurring in a short (6,5) tube because it is a one-time event and it is possible that a fraction of caps with 65 atoms (Figure 7) can react with C₂ despite the small reaction energy. But for caps (5,5), because the reaction energy changes periodically, the growth limitation will repeat periodically, thus reducing the chances of growing long (5,5) nanotubes.

To estimate the ability to grow of different caps, we compared the reaction energy of one period of cap-ended nanotubes (5,5) and (6,6) with the stable reaction energy of nanotube (6,5), as shown in Table 2. The average value of the adsorption energy follows the trend: cap (5,5) < cap (6,5) < cap(6,6); i.e., the adsorption strength increases with the nanotube diameter, which may be due to the effect of the reduction of the curvature energy as the diameter increases. However, the adsorption energy of cap-ended nanotubes (5,5) and (6,6) shows large variations when the number of carbon atoms in the nanotube increases. Therefore, for a particular type of nanotube, the smallest value of the reaction energy (weakest adsorption energy) may be taken as an indicator of the difficulty of the nanotube to grow. Thus, based on our calculations, the smallest value of the adsorption energy follows the trend cap (5,5) < cap(6,6) < cap(6,5). It is suggested that this may be at least one of the reasons why only a small percent of the nanotubes grown experimentally belong to the armchair type.

We remark that our analysis is purely thermodynamic and that entropic effects are ignored, and we acknowledge that the thermodynamic criterion does not provide any indication about the reaction kinetics.

4. Conclusions

The energy variation of the frontier molecular orbitals of capped single-wall carbon nanotubes of different chiralities as a function of the number of carbon atoms in the nanotube is correlated with the reaction energy released in the adsorption of a C₂ radical. An oscillatory behavior as a function of the number of carbon atoms is observed in the orbital energies of the armchair cap-ended SWNTs, which is reflected in oscillations in the reaction energy. In contrast, the chiral (6,5) cap-ended SWNT shows a more stable behavior as the number of C atoms in the nanotube increases, suggesting that this may be a reason for the selective production of chiral tubes found in catalyzed synthesis.

Acknowledgment. This work is partially supported by the National Science Foundation, grant NER/CTS-04003651.

References and Notes

- (1) Hafner, J. H.; Bronikowski, M. J.; Azamian, B. R.; Nikolaev, P.; Rinzler, A. G.; Colbert, D. T.; Smith, K. A.; Smalley, R. E. Catalytic growth of single-wall carbon nanotubes from metal particles. *Chem. Phys. Lett.* **1998**, *296*, 195–202.
- (2) Resasco, D. E.; Alvarez, W. E.; Pompeo, F.; Balzano, L.; Herrera, J. E.; Kitiyanan, B.; Borgna, A. A scalable process for production of single-walled carbon nanotubes (SWNTs) by catalytic disproportionation of CO on a solid catalyst. *J. Nanoparticle Res.* **2002**, *4*, 131–136.
- (3) Huang, S.; Woodson, M.; Smalley, R.; Liu, J. Growth mechanism of oriented long single walled carbon nanotubes using “fast-heating” chemical vapor deposition process. *Nano Lett.* **2004**, *4*, 1025–1028.
- (4) Gavillet, J.; Thibault, J.; Stephan, O.; Amara, H.; Loiseau, A.; Bichara, C.; Gaspard, J.-P.; Ducastelle, F. Nucleation and growth of single-walled nanotubes: The role of metallic catalysts. *J. Nanosci. Nanotech.* **2004**, *4*, 346–359.
- (5) Alvarez, W. E.; Pompeo, F.; Herrera, J. E.; Balzano, L.; Resasco, D. E. Characterization of single-walled carbon nanotubes (SWNTs) produced by CO disproportionation on Co–Mo catalysts. *Chem. Mater.* **2002**, *14*, 1853–1858.
- (6) Jorio, A.; Santos, A. P.; Ribeiro, H. B.; Fantini, C.; Souza, M.; Vieira, J. P. M.; Furtado, C. A.; Jiang, J.; Saito, R.; Balzano, L.; Resasco, D. E.; Pimenta, M. A. Quantifying carbon-nanotube species with resonance Raman scattering. *Phys. Rev. B* **2005**, *72*, 075207.
- (7) Zhang, L.; Balzano, L.; Resasco, D. E. Single-Walled Carbon Nanotubes of Controlled Diameter and Bundle Size and Their Field Emission Properties. *J. Phys. Chem. B* **2005**, *109*, 14375–14381.
- (8) Hennrich, F.; Krupke, R.; Lebedkin, S.; Arnold, K.; Fischer, R.; Resasco, D. E.; Kappes, M. M. Raman Spectroscopy of Individual Single-Walled Carbon Nanotubes from Various Sources. *J. Phys. Chem. B* **2005**, *109*, 10567–10573.
- (9) Zhao, J.; Martinez-Limia, A.; Balbuena, P. B. Understanding catalyzed growth of single-wall carbon nanotubes. *Nanotechnology* **2005**, *16*, S575–S581.
- (10) Balbuena, P. B.; Zhao, J.; Huang, S.; Wang, Y.; Sakulchaicharoen, N.; Resasco, D. E. Role of the catalyst in the growth of single-wall carbon nanotubes. *J. Nanosci. Nanotech.*, in press.
- (11) Ding, F.; Bolton, K.; Rosen, A. Nucleation and growth of single-walled carbon nanotubes: A molecular dynamics study. *J. Phys. Chem. B* **2004**, *108*, 17369–17377.
- (12) Gavillet, J.; Loiseau, A.; Ducastelle, F.; Thair, S.; Bernier, P.; Stephan, O.; Thibault, J.; Charlier, J. C. Microscopic mechanisms for the catalyst assisted growth of single-wall carbon nanotubes. *Carbon* **2002**, *40*, 1649–1663.
- (13) Lu, X.; Chen, Z. Curved pi-conjugation, aromaticity, and the related chemistry of small fullerenes (<C₆₀) and single-walled carbon nanotubes. *Chem. Rev.* **2005**, *105*, 3643–3696.
- (14) Bachilo, S. M.; Balzano, L.; Herrera, J. E.; Pompeo, F.; Resasco, D. E.; Weisman, R. B. Narrow (n, m)-Distribution of Single Walled Carbon Nanotubes Grown using a Solid Supported Catalyst. *J. Am. Chem. Soc.* **2003**, *125*, 11186–11187.
- (15) Frisch, M. J.; Trucks, G. W.; Schlegel, H. B.; Scuseria, G. E.; Robb, M. A.; Cheeseman, J. R.; Montgomery, J. A.; Vreven, T.; Kudin, K. N.; Burant, J. C.; Millam, J. M.; Iyengar, S. S.; Tomasi, J.; Barone, V.; Mennucci, B.; Cossi, M.; Scalmani, G.; Rega, N.; Petersson, G. A.; Nakatsuji, H.; Hada, M.; Ehara, M.; Toyota, K.; Fukuda, R.; Hasegawa, J.; Ishida, M.; Nakajima, T.; Honda, Y.; Kitao, O.; Nakai, H.; Klene, M.; Li, X.; Knox, J. E.; Hratchian, H. P.; Cross, J. B.; Bakken, V.; Adamo, C.; Jaramillo, J.; Gomperts, R.; Stratmann, R. E.; Yazyev, O.; Austin, A. J.; Cammi, R.; Pomelli, C.; Ochterski, J. W.; Ayala, P. Y.; Morokuma, K.; Voth, G. A.; Salvador, P.; Dannenberg, J. J.; Zakrzewski, V. G.; Dapprich, S.; Daniels, A. D.; Strain, M. C.; Farkas, O.; Malick, D. K.; Rabuck, A. D.; Raghavachari, K.; Foresman, J. B.; Ortiz, J. V.; Cui, Q.; Baboul, A. G.; Clifford, S.; Cioslowski, J.; Stefanov, B. B.; Liu, G.; Liashenko, A.; Piskorz, P.; Komaromi, I.; Martin, R. L.; Fox, D. J.; Keith, T.; Al-Laham, M. A.; Peng, C. Y.; Nanayakkara, A.; Challacombe, M.; Gill, P. M. W.; Johnson, B.; Chen, W.; Wong, M. W.; Gonzalez, C.; Pople, J. A. *Gaussian03*, revision C.02 ed.; Gaussian, Inc.: Wallingford, CT, 2004.
- (16) Matsuo, Y.; Tahara, K.; Nakamura, E. Theoretical studies on structures and aromaticity of finite-length armchair carbon nanotubes. *Org. Lett.* **2003**, *5*, 3181–3184.
- (17) Bulusheva, L. G.; Okotrub, A. V.; Romanov, D. A.; Tomanek, D. Electronic Structure of (n, 0) Zigzag Carbon Nanotubes: Cluster and Crystal Approach. *J. Phys. Chem. A* **1998**, *102*, 975–981.
- (18) Jensen, F. *Introduction to Computational Chemistry*; Wiley: Chichester, U.K., 1999.